PCCP

Cite this: *Phys. Chem. Chem. Phys.*, 2012, **14**, 3083–3088

www.rsc.org/pccp

PAPER

Efficient reduction of graphene oxide catalyzed by copper

Yu-Chuan Lin,[ab] Keng-Ku Liu,[a] Chih-Yu Wu,[a] Chih-Wei Chu,[a] Jacob Tse-Wei Wang,[a] Chi-Te Liang*[b] and Lain-Jong Li*[ac]

Received 9th October 2011, Accepted 20th December 2011
DOI: 10.1039/c2cp23187e

We report that copper thin films deposited on top of graphene oxide (GO) serve as an effective catalyst to reduce GO sheets in a diluted hydrogen environment at high temperature. The reduced GO (rGO) sheets exhibit higher effective field-effect hole mobility, up to 80 $cm^2\ V^{-1}\ s^{-1}$, and lower sheet resistance (13 $k\Omega\ \square^{-1}$) compared with those reduced by reported methods such as hydrazine and thermal annealing. Raman and XPS characterizations are addressed to study the reduction mechanism on graphene oxide underneath copper thin films. The level of reduction in rGO sheets is examined by Raman spectroscopy and it is well correlated with hole mobility values. The conductivity enhancement is attributed to the growth of the graphitic domain size. This method is not only suitable for reduction of single GO sheets but also applicable to lower the sheet resistance of Langmuir–Blodgett assembled GO films.

1. Introduction

Exfoliation or chemical oxidation of graphite in liquid phase has been a trend for the mass production of graphene thin sheets in recent years due to its simplicity, reliability, capability of large-scale production, relatively low materials cost, and versatility in terms of being well-suited for chemical functionalization.[1–7] However, oxidation by chemical methods introduces a variety of defects and oxygen-containing functional groups such as hydroxyl, carboxylic and epoxide groups in graphene; thus, it is called graphene oxide (GO). The electronic properties are severely degraded; therefore, a reduction process is required to recover the graphene structure and electrical properties. There have been reports on the reduction of GO, including chemical routes,[8–14] thermal annealing,[15–18] and photocatalytic reduction.[19] The reduction of GO is essentially related to the removal of the above mentioned functional groups.[20–25] However, due to the difficulty in fully recovering its graphitic structure, the field effect mobility is much lower than that of pristine graphene.[26–29] In this contribution, we observe that a thin layer of Cu film deposited on top of GO, subject to thermal annealing in the presence of hydrogen, is not only capable of removing the chemical functional groups, but also efficiently healing the graphitic structure in GO sheets. The increase in graphitic domain size after the Cu-assisted reduction, which in turn leads to enhancement in their electrical conductivity, has been verified by Raman measurements. This reduction method provides a new route to obtain not only highly conductive transparent electrodes with sheet resistance around 14 $k\Omega\ \square^{-1}$ (over 90% transparency at 550 nm) but also a high effective hole mobility, up to 80 $cm^2\ V^{-1}\ s^{-1}$.

[a] *Research Center for Applied Sciences, Academia Sinica, Taipei 11529, Taiwan. E-mail: lanceli@gate.sinica.edu.tw*
[b] *Department of Physics, National Taiwan University, Taipei 106, Taiwan. E-mail: ctliang@phys.ntu.edu.tw*
[c] *Department of Photonics, National Chiao Tung University, HsinChu 300, Taiwan*

2. Experimental section

2.1 Preparation of graphene oxide sheets

Graphene oxide (GO) sheets were prepared by the modified Hummer's method from natural graphite flakes (average size is 3–5 mm, from NGS Naturgraphit GmbH, Leinburg, Germany). The modified Hummer's method reported by Su *et al.*[3] was used in this experiment, in which the first step (the chemical oxidation of graphite flakes using concentrated H_2SO_4, P_2O_5, and $K_2S_2O_8$) was replaced with a bath sonication process. The sonication period strongly affects the size of the monolayered GO obtained. The subsequent oxidation process allows us to obtain fairly large size (more than 20 μm in lateral size) GO sheets, which makes the preparation of devices for electrical measurement easier than that with the small size GO.

2.2 Reduction of graphene oxide by using copper thin film

Single-layer GO films were deposited onto the silicon substrates with 300 nm silicon oxide by the dip-coating method. A 300 nm copper thin film was thermally deposited onto these samples by using a thermal evaporator at a pressure of 5×10^{-6} Torr. Thereafter, firstly the samples were loaded into a tube furnace (TF55030A, Lindberg/Blue M), and forming gas (H_2 at 415 sccm and Ar at 400 sccm) was introduced into the tube to purge undesired moisture and oxygen. Secondly the quartz tube was heated to 700 °C–900 °C, followed by dwelling for 10 to 15 min in a H_2 environment. Thirdly the furnace was cooled down to

room temperature at a rate of 10 °C–20 °C per second. After the thermal annealing process, the copper thin films were etched away in $FeCl_3$ solution and rinsed several times in DI water.

2.3 Fabrication of field-effect transistor devices

Single-layer GO films were deposited onto the silicon substrates with a 300 nm silicon oxide layer by the dip-coating method, followed by reduction underneath a 300 nm copper thin film. The dip-coating condition was tuned till loosely distributed GO sheets were deposited on substrates. The field-effect transistor device was fabricated by evaporating Au electrodes (50 nm thick) and Cr as the adhered layer (1 nm thick) directly on top of the selected, regularly shaped reduced GO sheets using a copper grid (200 mesh, 20 μm spacing) as a hardmask. The typically obtained channel length between source and drain electrodes was around 20–30 μm.

2.4 Preparation of thin-film electrodes

Quartz substrates were cleaned and made hydrophilic by a standard Piranha process. The Langmuir–Blodgett assembly method was employed to deposit GO sheets on quartz. Briefly, quartz substrates for receiving GO sheets were immersed in an aqueous GO suspension (0.062 mg mL^{-1}), followed by slow pulling (0.16 mm s^{-1}). Then, the substrates were dried in air followed by the alcohol reduction processes. A 300 nm copper thin film was deposited onto the GO thin films by using a thermal evaporator. Thermal-annealing at elevated temperature under H_2 was then applied to the GO thin films.

2.5 Characterization

The AFM images were obtained using a Veeco Dimension-Icon system. Raman spectra were collected in a NT-MDT confocal Raman microscopic system (laser wavelength 473 nm and laser spot-size is around 0.5 μm). The Si peak at 520 cm^{-1} was used as reference for wavenumber calibration. The UV-vis-NIR transmittance spectra were obtained using a Dynamica PR-10 spectrophotometer. Sheet resistance was measured using a four point probe system (PXI-1033, Super Solution & Services). XPS measurements were carried out using a Theta 300 X-ray photoelectron spectrometer (Thermo Scientific, the beam size is around 3 mm). The electrical measurements were performed under ambient conditions using a Keithley-4200 semiconductor analyzer.

3. Results and discussion

The as-prepared GO sheets were first dip-coated onto 300 nm SiO_2/Si substrates and then a layer of 300 nm Cu film was thermally evaporated on them, as schematically illustrated in Fig. 1. The reduction was performed by placing these samples in a hydrogen environment at various temperatures. After thermal reduction, the Cu capping layer was etched away in a $FeCl_3$ solution followed by rigorous rinsing with deionized water. Fig. 2a displays the typical atomic force microscopy (AFM) image of the GO on a SiO_2/Si substrate before reduction, the lateral size of the GO sheet normally ranged from 20 to 100 μm and its thickness was around 1.0 nm, suggesting that it was a monolayer GO sheet.

Using Cu as a catalytic template for synthesizing graphene by chemical vapor deposition (CVD) has been reported.[30–33] In these techniques, carbon-containing gas species are reacted

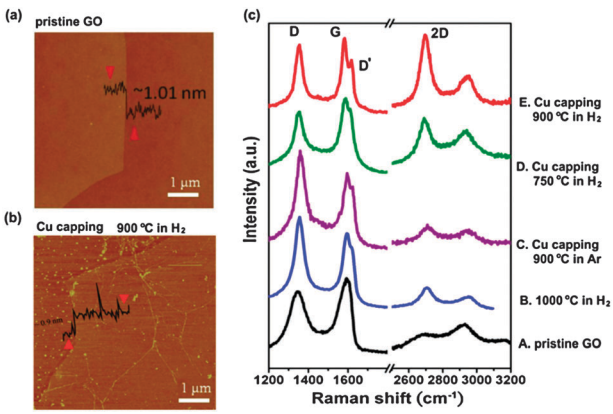

Fig. 2 AFM images of the GO sheets (a) before and (b) after reduction in H_2 at 900 °C in the presence of a 300 nm Cu capping layer, followed by Cu removal. (c) Raman spectra of the monolayer GO sheets before (curve A) and after various reduction procedures, including H_2 annealing without Cu capping (1000 °C in 20% H_2/Ar; curve B), reduction with Cu capping at 900 °C (in Ar; curve C), at 750 °C in H_2 (curve D) and at 900 °C in H_2 (curve E).

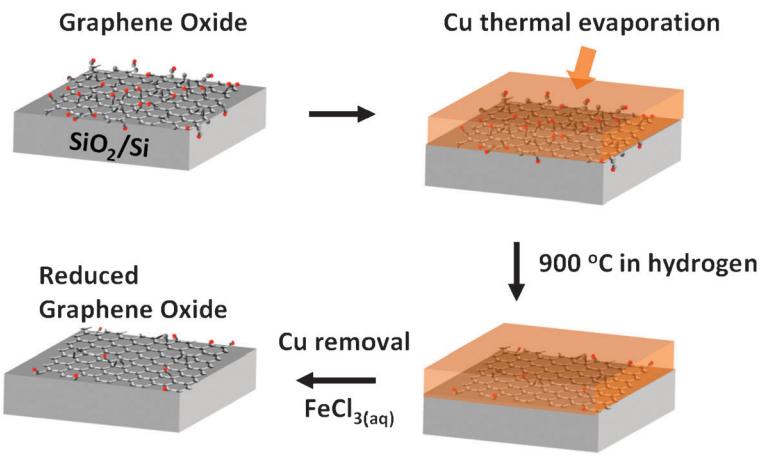

Fig. 1 Schematic illustration of the Cu-assisted method for graphene oxide reduction.

at high-temperature (900–1030 °C) in the presence of Cu thin film or foils, which serves two functions: the decomposition of carbon species and the nucleation and growth of graphene. The mechanism of graphene growth on a metal catalyst is presumably determined by many factors, including the carbon solubility in the metal, the crystal structure of the metal and process parameters such as temperature, pressure, and reaction gases. Here, instead of growing CVD graphene on top of Cu surfaces, the Cu thin film is adopted to reduce the underlying GO sheets. Fig. 2b shows the AFM image of the GO sheet after reduction in H_2 at 900 °C in the presence of a 300 nm Cu capping layer, followed by Cu removal. Note that 300 nm (or thicker) Cu is necessary for maintaining the continuity and uniformity of Cu film at high temperature.[31] Some wrinkles are observed in the topographic image but the film still remains as a monolayer. To reveal the effect of a Cu capping layer on GO reduction, in Fig. 2c the Raman spectra of the monolayer GO sheets before (curve A) and after various reduction procedures, including H_2 annealing without Cu capping (1000 °C in 20% H_2/Ar; curve B), reduction with Cu capping at 900 °C (in Ar; curve C), at 750 °C in H_2 (curve D) and at 900 °C in H_2 (curve E), are compared. The G peak at around 1580 cm^{-1} and the 2D peak at around 2680 cm^{-1} are typical features of the sp^2-hybridized carbon–carbon bonds in graphene.[34,35] Note that the Raman D band (~1350 cm^{-1}) and D' band (~1620 cm^{-1}) indicate the presence of defects.[34] The ratio of the integrated Raman peak area between the 2D and G bands, $I(2D)/I(G)$, has been shown to relate to the degree of recovery of sp^2 C=C bonds in graphitic structures.[35] Fig. 2c clearly shows that the $I(2D)/I(G)$ for the GO after reduction in H_2 with the Cu capping is much higher than that without Cu capping. Also, the ratio $I(2D)/I(G)$ of the GO reduced at 900 °C with Cu capping (curve E) can even reach 1.74. Meanwhile, based on the curves D and E, the reduction at 900 °C is better than at 750 °C. It is noted that the reduction at 750 °C in H_2 with Cu capping is readily much better than the case at 900 °C in an Ar-only environment with Cu capping, suggesting that H_2 plays a significant role in GO reduction. It is likely that H_2 not only removes the oxygen-containing functional groups in GO but also possibly activates the catalytic property of Cu.[32,36] The reduction of GO in an Ar-only environment (curve C) is not efficient likely due to the existence of copper or cuprous oxides, which deteriorates the catalytic property of Cu. Based on our previous report,[26] such a high $I(2D)/I(G)$ ratio indicates that the reduction not only involves the removal of functional groups but also the increase in graphitic domain size. In other words, the reduction of GO with the aid of Cu capping is able to achieve the restoration or repairing of graphitic structure. We hypothesize that the hydrogen-activated Cu surface promotes the reorganization of carbon atoms, and thus recrystallization of the graphitic domains. Fig. 3a and b, respectively, show the X-ray photoemission spectroscopy (XPS) results for the GO sheets before and after reduction at 900 °C in H_2 with Cu capping.

The XPS spectrum of the pristine GO consists of an intense C–O peak. It is obvious that the C–O bonding has been largely suppressed after reduction. To further confirm the restoration of graphitic structures in GO sheets by copper thin films, bottom-gate operated field-effect transistors were fabricated by evaporating Au electrodes directly on top of the reduced

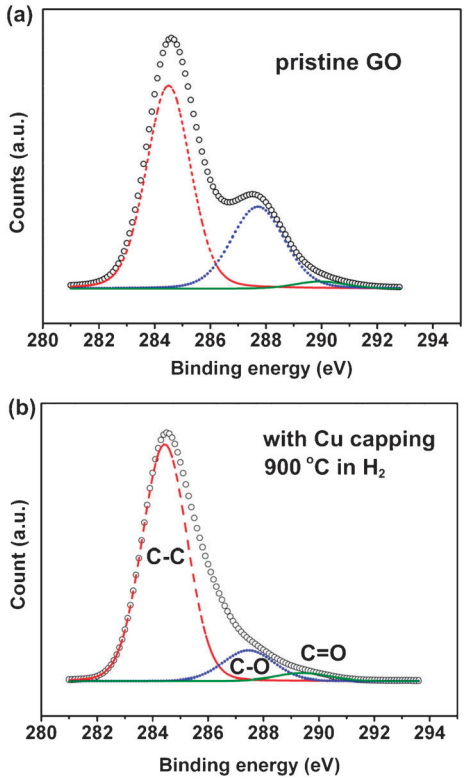

Fig. 3 X-Ray photoemission spectroscopy (XPS) results for the GO sheets (a) before and (b) after reduction at 900 °C in H_2 with Cu capping.

GO sheets, which were previously deposited on SiO_2/Si substrates. The device structure is illustrated in Fig. 4a. Fig. 4b shows the transfer curves (drain current I_d *vs.* gate voltage V_g) for the device prepared from a monolayered GO sheet after the reduction at 900 °C. The charge neutrality point is observed at 90 V for the as-prepared device and the *p*-type behaviour is readily achieved as well. The field-effect mobility of holes for this device is around 80 $cm^2\ V^{-1}\ s^{-1}$, which is 2 orders of magnitude higher than the reported around 0.01–1 $cm^2\ V^{-1}\ s^{-1}$ after the reduction using hydrazine vapor reduction.[27,28] The value was extracted based on the slope, $\Delta I_d/\Delta V_g$, which was fitted to the linear regime of the transfer curve using the equation: $\mu = (L/WC_{ox}V_d)(\Delta I_d/\Delta V_g)$,[37] where L and W are the channel and width, and C_{ox} is the gate capacitance. Fig. 4c demonstrates the output characteristics (drain current I_d *vs.* drain voltage V_d) of the device. It is worthy of note that more than 40 devices were tested to confirm the electrical output performance, with all measurements carried out under ambient conditions. Fig. 4d compiles the field-effect mobility data for the devices made from the monolayered GO sheets reduced at 900 °C in H_2 with Cu capping, the devices reduced at 1000 °C in H_2 without Cu capping, and the devices reduced from hydrazine vapors. The statistical results show that the mobility of GO sheets from Cu-assisted reduction achieves 56 $cm^2\ V^{-1}\ s^{-1}$ in average, which is comparable to that of those reduced in the presence of extra carbon sources.[26,38] Furthermore, the device mobility for the GO sheet from Cu-assisted reduction at 900 °C is even higher than that of those reduced in H_2 at 1000 °C without Cu capping, corroborating that Cu plays a role in recovering graphitic structure of the sheets.

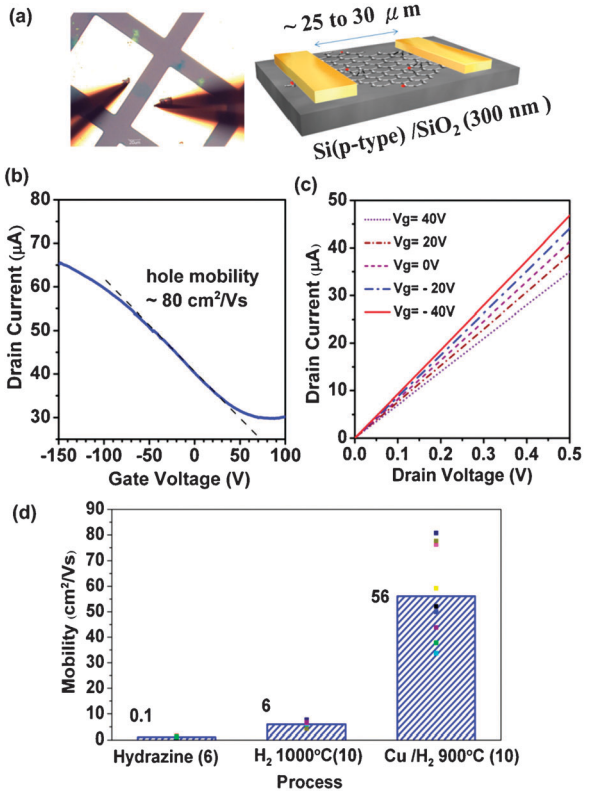

Fig. 4 (a) The structure of the field-effect transistor made from the reduced GO sheets. (b) The transfer curves (drain current I_d *vs.* gate voltage V_g) for the device prepared from a monolayered GO sheet after the reduction at 900 °C. (c) The output characteristics (drain current I_d *vs.* drain voltage V_d) of the device. (d) The statistical mobility results for the devices made from the monolayered GO sheets reduced at 900 °C in H_2 with Cu capping, the devices reduced at 1000 °C in H_2 without Cu capping, and the devices reduced from hydrazine vapors. The numbers in parentheses indicate the number of devices prepared.

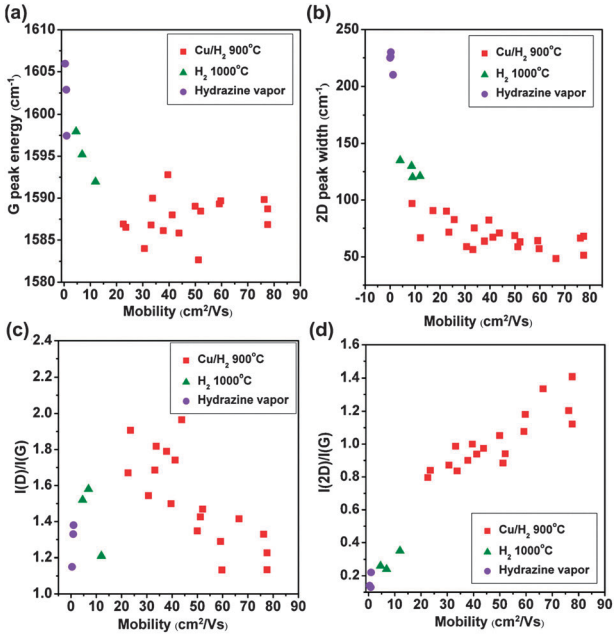

Fig. 5 The correlations of field-effect mobility of the GO reduced by the specified methods with several Raman features: (a) G band energy, (b) 2D peak width, (c) integrated ratios of I(D)/I(G) and (d) I(2D)/I(G), .

To correlate the electrical properties of the single GO sheets with their structural changes, confocal Raman spectroscopy was adopted to characterize the GO sheets reduced by various methods in the field-effect transistor devices. The mobility values were used as the indices for the degree of graphitic structure restoration, as in previous reports.[26,38] The Raman spectra of the devices were collected after the electrical measurement. The correlations of several Raman features, integrated ratios of I(D)/I(G) and I(2D)/I(G), to the field-effect mobility are shown in Fig. 5. Note that the Raman feature or field effect mobility naturally shows a distribution for each reduction method. The Raman D, G and 2D peaks in each spectrum were fitted with Lorentzian peaks. According to the previous reports, GO sheets display a prominent G peak at around 1593 cm^{-1}–1606 cm^{-1} before reduction.[26,39–40] It has been reported that the decrease in G band energy indicates the development of long-range and in-plane graphene order.[41–44] Fig. 5a shows that the G peak position of the Cu-reduced GO sheets has shifted to a lower wavenumber, 1587 cm^{-1}, suggesting the efficient recovery of the graphene structure while G peaks of the rGO derived from hydrazine vapor and hydrogen annealing at 1000 °C are still maintained at a relatively higher wavenumber. Furthermore, the decrease of the 2D peak width has been used to indicate the restoration of graphitic structures in graphite.[35] Fig. 5b shows that the 2D peak width decreases from the low mobility regime, including those reduced by hydrazine vapor and those reduced at 1000 °C in H_2, and then approaches 50 cm^{-1} in the higher mobility regime, corresponding to the evolution of the G peak frequency in Fig. 5a. The evolution of I(D)/I(G) with mobility helps to provide structural information of the GO with different degrees and various processes of reduction, as shown in Fig. 5c. Ferrari *et al.* have reported that the development of Raman D peak indicates not only disordering of graphite but also ordering of amorphous carbon structures.[42,43] For highly disordered structures, such as amorphous carbon or low mobility GO, the probability of existence of a six-fold ring in the cluster is low and the intensity of the D peak is related to the richness of the six-fold aromatic ring. Meanwhile, the G peak is caused by in-plane bond stretching of pairs of sp^2 carbon atoms, and it occurs at all sp^2 sites and is not essentially related to the presence of a six-fold ring. As shown in Fig. 5c, I(D)/I(G) increases with the mobility for GO reduced from hydrazine vapor and those reduced at 1000 °C in H_2 in the low mobility regime (0–10 $cm^2\ V^{-1}\ s^{-1}$). Once the GO is further reduced I(D)/I(G) decreases with decreasing disorder in graphitic structures. Fig. 5d shows that the ratio I(2D)/I(G) of the reduced GO sheets increases from the low mobility regime to the high mobility regime. Combining G peak downshift and the increase in the I(2D)/I(G) ratio suggests that the reduced graphene oxide exhibits a p-type behaviour,[44,45] and sp^2 C=C bonds (graphitization) in graphitic structures of reduced GO are efficiently recovered.[46]

The Cu-assisted reduction method is not only suitable for single GO sheets but also applicable to the assembled GO films. Here, the GO sheets were deposited onto quartz substrates using the Langmuir–Blodgett assembly method.[47,48] Fig. 6a shows the

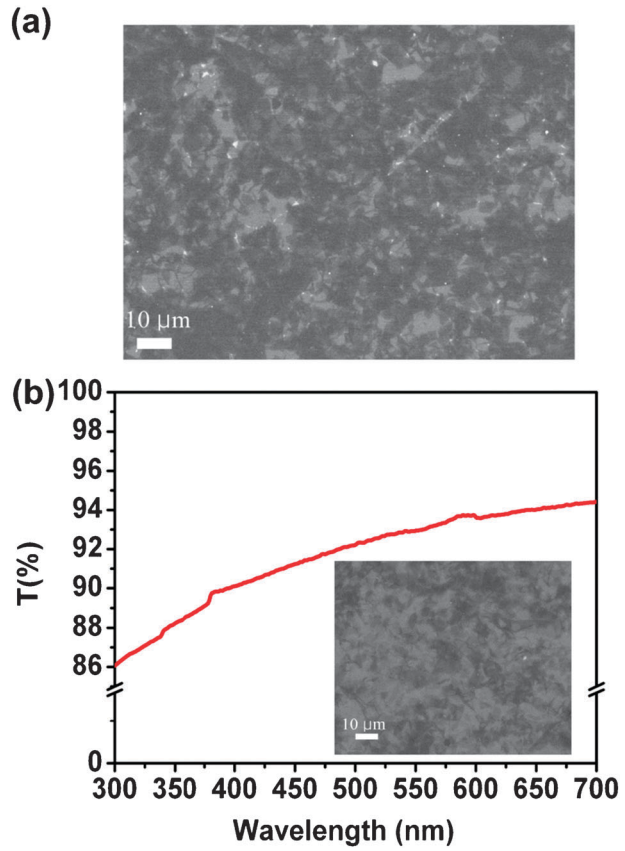

Fig. 6 (a) SEM for the as-prepared transparent thin films assembled from the pristine GO sheets using the Langmuir–Blodgett method. (b) Optical transmittance curve for the film after Cu-assisted reduction at 900 °C. Inset shows the SEM for the reduced film.

Table 1 Comparison of ultra-thin electrodes prepared from GO by various methods

Sample ID	Process	Transparency (% @550 nm)	Sheet resistance/kΩ □$^{-1}$
1[a]	20% H_2/Ar with alcohol 900 °C, 30 min	98.2	43
2[b]	20% H_2/Ar 900 °C, 2 h	98.1	413
3[a]	20% H_2/Ar with alcohol 1000 °C, 30 min	96.2	15
4[b]	20% H_2/Ar 1000 °C, 2 h	98.0	188
5[c]	Vacuum annealing 1100 °C, 3 h	95.0	500
6[d]	Hydrazine vapor reduction	95.4	19 000
7[e]	100% H_2 with Cu capping 900 °C, 10 min	93.4	13.9

[a] From ref. 26. [b] From ref. 3. [c] From ref. 18. [d] From ref. 47. [e] This work.

scanning electron microscopy (SEM) image of the assembled transparent thin film before reduction. Fig. 6b shows that the morphology of the Cu-reduced transparent thin films retained good uniformity, and the transmittance of the film is over 90% spanning from 390 nm to 750 nm. Table 1 shows that the GO transparent film reduced by various processes exhibits a high sheet resistance (200 kΩ □$^{-1}$–19 000 kΩ □$^{-1}$).[3,18,26,47] It is noted that the sheet resistance of GO films after 900 °C reduction with Cu capping is relatively low (13.9 kΩ □$^{-1}$), and the thin film exhibits similar transparency (T = 90–96%). Also, the sheet resistance of 13.9 kΩ □$^{-1}$ is comparable to 500 kΩ □$^{-1}$ obtained by vacuum annealing at 1100 °C,[18] and 15–43 kΩ □$^{-1}$ obtained by alcohol-reduced GO films.[26]

4. Conclusions

Our results show that with the copper films serving as a catalytic layer, the GO sheets can be efficiently reduced through the thermal annealing process. The conductivity enhancement is attributed to the growth of the graphitic domain size with the help from copper, which catalyzes the restoration of the graphene lattice. The proposed method enhances the electrical conductivity of GO and restores its graphitic domain merely with a thin copper film without the need for extra carbon precursors. This method is not only suitable for reduction of single GO sheets but also applicable to lower the sheet resistance of Langmuir–Blodgett assembled GO films.

Acknowledgements

This research was supported by Research Center for Applied Sciences, Academia Sinica Nano Program and National Science Council Taiwan (NSC-99-2112-M-001-021-MY3, 99-2738-M-001-001 and National science and technology project). We also thank Prof. J. Huang and L. Cote (Northwestern Univ., USA) for useful discussions and comments.

References

1 Y. Hernandez, V. Nicolosi, M. Lotya, F. M. Blighe, Z. Sun, S. De, I. T. McGovern and B. Holland, *Nat. Nanotechnol.*, 2008, **3**, 563.
2 H. C. Schniepp, J.-L. Li, M. J. McAllister, H. Sai, M. Herrera-Alonso, D. H. Adamson, R. K. Prud'homme, R. Car, D. A. Saville and I. A. Aksay, *J. Phys. Chem. B*, 2006, **110**, 8535.
3 C.-Y. Su, Y. P. Xu, W. J. Zhang, C. H. Tsai, J. W. Zhao, X. H. Tang and L.-J. Li, *Chem. Mater.*, 2009, **21**, 5674.
4 C.-Y. Su, A.-Y. Lu, Y. Xu, F.-R. Chen, A. N. Khlobystov and L.-J. Li, *ACS Nano*, 2011, **5**, 2332.
5 E.-K. Choi, I.-Y. Jeon, S.-Y. Bae, H.-J. Lee, H.-S. Shin, S. L. Dai and J.-B. Baek, *Chem. Commun.*, 2010, **46**, 6320.
6 X. Huang, X. Qi, F. Boey and H. Zhang, *Chem. Soc. Rev.*, 2012, **41**, 666.
7 X. Huang, Z. Yin, S. Wu, X. Qi, Q. He, Q. Zhang, Q. Yan, F. Boey and H. Zhang, *Small*, 2011, **7**, 1786.
8 S. Stankovich, D. A. Dikin, R. D. Piner, K. A. Kohlhass, A. Kleinhammes, Y. Jia, Y. Wu, S. T. Nguyen and R. S. Rouff, *Carbon*, 2007, **45**, 1558.
9 D. Li, M. B. Müller, S. Gilje, R. B. Kaner and G. G. Wallace, *Nat. Nanotechnol.*, 2008, **3**, 101.
10 L. J. Cote, R. Cruz-Silva and J. Huang, *J. Am. Chem. Soc.*, 2009, **131**, 11027.
11 Q. He, S. Wu, S. Gao, X. Cao, Z. Yin, H. Li, P. Chen and H. Zhang, *ACS Nano*, 2011, **5**, 5038.
12 B. Li, X. Cao, H. K. Ong, J. W. Cheah, X. Zhou, Z. Yin, H. Li, J. Wang, F. Boey, W. Huang and H. Zhang, *Adv. Mater.*, 2010, **22**, 3058.
13 B. H. Kim, J. Y. Kim, S.-J. Jeong, J. O. Hwang, D. H. Lee, D. O. Shin, S.-Y. Choi and S.-O. Kim, *ACS Nano*, 2010, **4**, 5464.
14 S. Wu, Z. Yin, Q. He, G. Lu, Q. Yan and H. Zhang, *J. Phys. Chem. C*, 2011, **115**, 15973.
15 Z. Yin, S. Sun, T. Salim, S. Wu, X. Huang, Q. He, Y. M. Lam and H. Zhang, *ACS Nano*, 2010, **4**, 5263.
16 Z. Yin, S. Wu, X. Zhou, X. Huang, Q. Zhang, F. Boey and H. Zhang, *Small*, 2010, **6**, 307.

17 X. Li, H. Wang, J. T. Robinson, H. Sanzhez, G. Diankov and H. Dai, *J. Am. Chem. Soc.*, 2009, **131**, 15939.
18 H. Becerril, J. Mao, Z. Liu, R. M. Stoltenberg, Z. Bao and Y. Chen, *ACS Nano*, 2008, **2**, 463.
19 G. William, B. Seger and P. V. Kamat, *ACS Nano*, 2008, **2**, 1487.
20 X. Gao, J. Jang and S. Nagase, *J. Phys. Chem. C*, 2010, **114**, 832.
21 W.-F. Chen, L. Yan and P. R. Bangal, *J. Phys. Chem. C*, 2010, **114**, 19885.
22 K.-H. Liao, A. Mittal, S. Bose, C. Leighton, K. A. Mkhoyan and C. W. Macosko, *ACS Nano*, 2011, **5**, 1253.
23 W. Gao, L. B. Alemany, L. Ci and P. M. Ajayan, *Nat. Chem.*, 2009, **1**, 403.
24 Y. Zhou, Q. Bao, L. A. L. Tang, Y. Zhong and K. P. Loh, *Chem. Mater.*, 2009, **21**, 2950.
25 J. P. Rourke, P. A. Pandey, J. J. Moore, M. Bates, I. A. Kinloch, R. J. Young and N. R. Wilson, *Angew. Chem., Int. Ed.*, 2011, **50**, 3173.
26 C. Y. Su, Y. P. Xu, Y. P. Zhang, J. Zhao, A. Liu, X. Tang, C.-H. Tsai, Y. Huang and L.-J. Li, *ACS Nano*, 2010, **4**, 5285.
27 C. Gómez-Navarro, R. T. Weitz, A. M. Bittner, M. Scolari, A. Mews, M. Burgard and K. Kern, *Nano Lett.*, 2009, **9**, 2206.
28 G. Eda, C. Mattevi, H. Yamaguchi and H. Chhowalla, *J. Phys. Chem. C*, 2009, **114**, 15768.
29 D. Yang, A. Velamakanni, G. Bozoklu, S. Park, M. Stoller, R. D. Piner, S. Stankovich, I. Jung, D. A. Field, C. A. Ventrice, Jr. and R. S. Ruoff, *Carbon*, 2009, **47**, 145.
30 X. S. Li, W. Cai, J. An, S. Kim, J. Nah, D. Yang, R. Piner, A. Velamakanni, I. Jung, S. K. Banerjee, L. Colombo and R. S. Ruoff, *Science*, 2009, **324**, 1312.
31 A. Ismach, C. Druzgalski, S. Penwell, A. Schwartzberg, M. Zhang, A. Javey, J. Bokor and Y. Zhang, *Nano Lett.*, 2010, **10**, 1542.
32 I. Vlassiouk, M. Regmi, P. Fulvio, S. Dai, P. Daskos, E. Gyula and S. Smirnov, *ACS Nano*, 2011, **5**, 6069.
33 C.-Y. Su, A.-Y. Lu, C.-Y. Wu, Y.-T. Li, K.-K. Liu, W. Zhang, S.-Y. Lin, Z.-Y. Juang, Y.-L. Zhong, F.-L. Chen and L.-J. Li, *Nano Lett.*, 2011, **11**, 3612.
34 A. C. Ferrari, J. C. Meyer, V. Scardaci, M. Lazzeri, F. Mauri, S. Piscanec, D. Jiang, K. S. Novoselov, S. Roth and A. K. Geim, *Phys. Rev. Lett.*, 2006, **97**, 187401.
35 B. Krauss, T. Lohmann, D.-H. Chae, M. Haluska, K. von Klitzing and J. H. Smet, *Phys. Rev. B: Condens. Matter Mater. Phys.*, 2009, **79**, 165428.
36 H. Ji, Y. Hao, Y. Ren, M. Charlton, H. L. Wi, Q. Wu, H. Li, Y. Zhu, Y. Wu, R. Piner and R. S. Ruoff, *ACS Nano*, 2011, **10**, 1021.
37 D. L. Fu, H. Okimoto, C. W. Lee, T. Takenobu, Y. Iwasa, H. Kataura and L.-J. Li, *Adv. Mater.*, 2010, **22**, 4867.
38 V. López, R. S. Sundaram, C. Gómez-Navarro, D. Olea, M. Burgard, J. Gómez-Navarro, F. Zamora and K. Kern, *Adv. Mater.*, 2009, **21**, 4683.
39 X. Dong, C.-Y. Su, W. Zhang, J. Zao, Q. Ling, W. Huang, P. Chen and L.-J. Li, *Phys. Chem. Chem. Phys.*, 2010, **12**, 2164.
40 K. N. Kudin, B. Ozbas, H. C. Schniepp, R. K. Prud'homme, I. A. Aksay and R. Car, *Nano Lett.*, 2009, **8**, 36.
41 T. C. Chieu, M. S. Dresselhaus and M. Endo, *Phys. Rev. B*, 1982, **26**, 5867.
42 A. C. Ferrari, *Solid State Commun.*, 2007, **143**, 47.
43 M. A. Pimenta, G. Dresselhaus, M. S. Dresselhaus, L. G. Cançado, A. Jorio and R. Saito, *Phys. Chem. Chem. Phys.*, 2007, **9**, 1276.
44 X. C. Dong, W. J. Fang, D. L. Fu, Y. M. Shi, P. Chen and L.-J. Li, *Small*, 2010, **2**, 1422.
45 A. Das, S. Pisana, B. Chakraborty, S. Piscanec, S. K. Saha, U. V. Waghmare, K. S. Novoselov, H. R. Krishnamurthy, A. K. Geim, A. C. Ferrari and A. K. Sood, *Nat. Nanotechnol.*, 2008, **3**, 210.
46 J. Yan, Y. Zhang, P. Kim and A. Pinczuk, *Phys. Rev. Lett.*, 2007, **98**, 166802.
47 L. J. Cote, F. Kim and J. Huang, *J. Am. Chem. Soc.*, 2009, **131**, 1043.
48 L. J. Cote, J. Kim, Z. Zhang, C. Sun and J. Huang, *Soft Matter*, 2010, **6**, 6096.

